

Journal of Materials Chemistry C

Accepted Manuscript



This is an *Accepted Manuscript*, which has been through the Royal Society of Chemistry peer review process and has been accepted for publication.

Accepted Manuscripts are published online shortly after acceptance, before technical editing, formatting and proof reading. Using this free service, authors can make their results available to the community, in citable form, before we publish the edited article. We will replace this *Accepted Manuscript* with the edited and formatted *Advance Article* as soon as it is available.

You can find more information about *Accepted Manuscripts* in the [Information for Authors](#).

Please note that technical editing may introduce minor changes to the text and/or graphics, which may alter content. The journal's standard [Terms & Conditions](#) and the [Ethical guidelines](#) still apply. In no event shall the Royal Society of Chemistry be held responsible for any errors or omissions in this *Accepted Manuscript* or any consequences arising from the use of any information it contains.

Cite this: DOI: 10.1039/c0xx00000x

www.rsc.org/xxxxxx

ARTICLE TYPE

Optical modulation in microsized optical resonators with irregular hexagonal cross section

Hongxing Dong,^a Yang Liu,^a Shulin Sun,^{*b} Zhanghai Chen,^c and Long Zhang^{*a}

Optical resonant modes in microwire cavities with irregular hexagonal cross section have been observed in the visible spectral range. Single-crystalline In_2O_3 microwire functioned as a promising semiconductor microcavity, was fabricated by a simple sublimation-oxidation-deposition strategy. By using the spatially resolved spectroscopic technique, the effects of the cross sectional geometry on optical modulations were carefully investigated. The experimental results fit well with the plane wave interference model and Finite Element Method simulations. Our results demonstrate that the In_2O_3 microwire optical resonator offers another practical example for the study of the fundamental physics research in the field of cavity optics, and may be helpful for the development of the miniature cavity-based optoelectronic devices.

Introduction

Micro/nanostructures with high crystalline quality and regular geometrical shape as optical resonators have been attracting great attentions for their excellent optical properties and widely potential applications.¹⁻³ The microstructure itself functions as both the gain medium and the optical resonator. In the micro/nanostructure optical resonators, the propagation of light can be restricted and modulated in low dimensions, and the electromagnetic field of light can be precisely controlled, which are very important for both fundamental studies on quantum electrodynamics and the development of effectively nanoscale devices, such as microlasers,⁴ optical waveguides,³ tunable filters,⁵ and optical sensors.⁶ The strategy to realize a new and efficient optical resonator becomes the striving direction of many optics researchers. In 2004, Nobis's group reported for the first time that the ZnO nanowire whispering gallery mode (WGM) microcavity with regular hexagonal cross section.⁷ In this type of resonant model, lights can be completely confined by six boundaries and circulate around due to multiple total internal reflections, which can exhibit low loss and high quality factor. Such optical microcavities quickly attract people's great attention. Up to now, many micro/nanowires such as GaN,⁸ In_2O_3 ,⁹ ZnS,¹⁰ ZnO^{11-13} etc., have been developed. It has been demonstrated that the cross sectional geometry is a crucial factor to achieve effective modulation of light field in the microcavity. Further understanding the key factor and controlling them in a systematic

way are therefore interesting and important. However, so far, almost all of the studies about the micro/nanostructure WGM resonators are limited on those with regular hexagonal cross section, which is not conducive to further understanding and optimization optical modulations in low dimensions. It is believed that if the hexagonal cross section shape is not perfect, the resonant modes should be changed, and the irregular structure configuration is usually required in practical applications. Furthermore, because of the difficulty of the sample preparations, practical examples of micro/nanostructure in the form of irregular hexagonal WGM resonator are very rare. The understanding of the dependence of optical modulation on such classical hexagonal cross sectional shape has so far mainly been inferred from simple geometrical optics theory.

Indium oxide (In_2O_3) is a promising semiconductor oxide material with a wide bandgap for optoelectronic applications in the visible spectral range and widely studied in recent years. In_2O_3 nanostructures with different morphologies, such as nanobelts,¹⁴ nanowires,^{15,16} nanosheets,¹⁷ nanoparticles,^{18,19} etc., have been fabricated using various methods. However, most of the synthesized In_2O_3 nanostructures have poor crystal quality, rough surfaces and too small sizes, which lead to such important semiconductor material can not be applied in the field of optical cavity over a long period. Recently, our group firstly obtained In_2O_3 1D microwire WGM optical cavity using an in situ thermal oxidation method, exhibiting excellent performance of optical modulations.¹⁰ The results demonstrate that the cubic In_2O_3 material also can be grown into the single-crystalline nanowire with hexagonal cross section. However, compared with the traditional hexagonal crystal, the hexagonal symmetry of the cross section structure is not strictly in the In_2O_3 crystal growth process, which may open up the possibility of studying experimentally the effects of nanowire geometry on hexagonal WGM optical modulations.

In the present study, we develop a facile in situ sublimation-

^aKey Laboratory of Materials for High-Power Laser, Shanghai Institute of Optics and Fine Mechanics, Chinese Academy of Science, Shanghai 201800, China. E-mail: lzhang@siom.ac.cn

^bDepartment of Optical Science and Engineering and Shanghai Engineering Research Center of Ultra-Precision Optical Manufacturing, Fudan University, Shanghai 200433, China. E-mail: sls@fudan.edu.cn

^cState Key Laboratory of Surface Physics and Department of Physics, Fudan University, Shanghai 200083, China.

oxidation-deposition strategy for fabrication of high quality single-crystalline In_2O_3 microwires with irregular hexagonal cross sections. We find experimentally that such microwires also can effectively control the light field in two dimensions.

5 Compared with the conventional microwire cavity with regular cross section, the present irregular microwire cavity will exhibit quite different features for its optical resonant modes due to the distinct TIR angles and the broken hexagonal symmetry. Their optical modulations were observed at room temperature and mapped directly by using a spatially resolved spectroscopic technique. The results were compared with full-wave electromagnetic simulations, which both supported our experimental results and helped to clarify the nature of the resonance modes in the irregular hexagonal WGM cavities. The experiments and theoretical analyses indicate that the obtained In_2O_3 microwire resonator is a promising test-bed for investigating new optical modulation behavior and developing novel optical devices.

Experimental

20 Preparation

Single-crystalline In_2O_3 microwires with irregular hexagonal cross sections were synthesized in a conventional horizontal tube furnace using indium grain and O_2 vapor as the source material. No catalysts, carrier gases and low pressure were used in the reaction process. Prior to the synthesis, indium grains (purity of 99.999%) with diameter of 2~3 mm were treated in an aqueous 1.0 M HCl solution for 30 s and then cleaned with absolute ethanol in an ultrasonic bath for 10 min. The grain was loaded into a small quartz boat. The reaction boat was covered with a clean quartz wafer substrate, which can greatly improve the collection efficiency of the sample. Then, the boat was placed at the center of the quartz tube mounted in the furnace. Before heating, high-purity N_2 was introduced into the tube with a constant flow rate of 5.0 L/h to purge the air inside. After 30 min of purging, the furnace was heated to 900 °C for over 60 min with a constant flow of N_2 gas at a rate of 1.0 L/h. Afterward, 1.0 L/h O_2 vapor was introduced into the tube, and the reaction temperature was kept at 900 °C for 60 min. After the system cooled down to room temperature under a constant flow of N_2 gas at a rate of 1.0 L/h, a large quantity of crystal-like products was deposited on the surface of the boat and the top quartz wafer.

Characterization

The morphology, crystal structure and composition of the obtained products were characterized by field emission scanning electron microscopy (FESEM, Zeiss Auriga S40), high-resolution transmission electron microscopy (HRTEM, JEOL-2100), energy dispersion X-ray spectroscopy (EDS) and X-ray diffraction (XRD, Bruker D8 ADVANCE) with Cu-K α 1 ($\lambda=1.5406$ Å). Optical studies of individual In_2O_3 microwire optical cavity were carried out using a confocal micro-photoluminescence system (JY Lab RAM HR800 UV). A He-Cd laser at 325 nm was used as the excitation source. The excitation laser was focused onto the microwire with a spot size of 1~2 μm in diameter by a microscope objective (40X) and scanned at steps of 1.0 μm along the c-axis of the In_2O_3 microwire. Polarization-resolved PL was performed with TE and TM configurations. The electrical vector

of excitation laser E was always parallel to the c-axis. Theoretical simulations were performed using a commercial finite element software (COMSOL Multiphysics).

60 Results and discussion

Fig. 1(a) is a typical low-magnification SEM image of the as-prepared products. All microwires are neatly arranged and grown on the surface of the quartz wafer. The microwires have the length of about 80~120 μm and the diameter of smaller than 5 μm . The enlarged image in Fig. 1(b) shows that the microwire has a hexagonal cross section and smooth surfaces. The yield of the microwires was estimated at about 40% of the total product deposited on the sample substrate. The XRD pattern of the as-prepared microwires is shown in Fig. 1(c). All of the diffraction peaks in the XRD pattern can be indexed to a pure body-centered cubic (bcc) phase of In_2O_3 with lattice constant of $a = 10.12$ Å, consistent with the JCPDS card (89-4595). No impurity peaks can be detected, which indicates that the samples are pure In_2O_3 with the bcc structure. In addition, TEM analyses were performed to get further information about the microstructure of the In_2O_3 microwires. Fig. 1(d) shows the TEM image of one single In_2O_3 microwire, illustrating the uniform morphology and smooth surface. The EDS data (inset of Fig. 1(d)) of the In_2O_3 microwires indicate that the In_2O_3 microwire samples are indeed stoichiometric in composition. The Cu signal in the EDS spectrum comes from the grid used for TEM measurements. High resolution TEM image taken from the rectangular region marked in Fig. 1(d) and the corresponding selected area electron diffraction (SAED) pattern (inset in Fig. 1(e)) indicate that the obtained In_2O_3 microwires are single crystalline with bcc lattice and high quality.

Based on the above analyses of the morphology and structure, the obtained In_2O_3 microwire may be used as the classical WGM cavity with regular hexagonal cross section. A single In_2O_3 microwire was selected for the optical measurements. Fig. 2(a) shows the detailed geometrical morphology of one single In_2O_3 microwire dispersed onto a Si substrate. It can be seen that the microwire has flat and smooth hexagonal resonator facets. The excitation laser was focused on a 2 μm spot on the In_2O_3 microwire at the position marked by a red cross. To further obtain the accurate cross section structure and size of the detect position, the microwire was processed by focused ion beam etching as shown in Fig. 2(b). The inset shows the cross section of the etched part of In_2O_3 microwire observed by vertically rotating the sample. It is surprising to find that the prepared In_2O_3 microwires have irregular hexagonal cross sections, which are rarely studied and reported in previous literatures. One can see that the hexagonal cross section has two different side lengths, R_1 and R_2 . From the point of view of geometrical optics, four kinds of resonant cavity modes may be formed in the microwire resonator: (I) WGMs, a light wave confined within the hexagonal cross section with the angle of incidence of 54° and 66° (Fig. 2(c)); (II) cross-WGMs, the light ray strikes the boundary six times at an angle of incidence of 30° (Fig. 2(d)); (III) quasi-WGMs, formed in the three equal planes as shown in Fig. 2(e); (IV) FPMs, formed between the two opposite planes (Fig. 2(f)). Due to the large refractive index of In_2O_3 ($n \approx 2.0$) in the visible spectral range, the smallest angle of total internal reflection (TIR) is about 30°.

Theoretically, TIRs in the above mentioned resonant modes can be achieved in the microwire. Taking into account the number of TIRs and path length for each resonance mode, the effective length of the cavity L can be written as the following equations:

WGM:

$$L = \frac{\lambda}{N} \left[N + \frac{3}{\pi} \arctan \left(\beta \sqrt{\frac{n^2 \sin^2 \theta_1 - 1}{\cos^2 \theta_1}} \right) + \frac{3}{\pi} \arctan \left(\beta \sqrt{\frac{n^2 \sin^2 \theta_2 - 1}{\cos^2 \theta_2}} \right) \right] \quad (1)$$

Cross-WGMs:

$$L = \frac{\lambda}{N} \left[N + \frac{6}{\pi} \arctan \left(\beta \sqrt{\frac{n^2 - 4}{3}} \right) \right] \quad (2)$$

Quasi-WGMs:

$$L = \frac{\lambda}{N} \left[N + \frac{3}{\pi} \arctan \left(\beta \sqrt{\frac{n^2 - 4}{3}} \right) \right] \quad (3)$$

FPMs:

$$L = N \frac{\lambda}{n} \quad (4)$$

Where L is the effective length of the cavity, λ is the resonant mode wavelength, n is the refractive index of medium, N is the interference order, θ is the angle of incidence ($\theta_1=54^\circ$, $\theta_2=66^\circ$). The factor β denotes polarization, for TM polarization (the electrical component of light ($E \parallel c$ -axis) $\beta=1/n$, and for TE polarization ($E \perp c$ -axis) $\beta=n$.

Optical studies of the selected In_2O_3 microwire were carried out with a micro-confocal photoluminescence (PL) spectrometer. We performed PL measurements with detection of unpolarized, TM polarized and TE polarized signals. Fig. 3(a) shows the typical spectra of the In_2O_3 microwire in the visible region. It can be seen that three different PL signals in the range of 450-750 nm with clear modulations were obtained. The physical origin of the visible emission is mainly attributed to indium vacancies or oxygen related defects.^{20,21} The obtained distinct modulations should correspond to the optical resonant modes induced by the microwire cavity. The unpolarized signal is dominated by the TM component, and both TM and TE polarized modes are clearly present. In addition, some other resonant modes also can be detected, which are preferentially TM polarized. The results are different from the previous investigations of traditional WGMs in In_2O_3 microcavities.⁹

In optical microcavities, the resonant mode spacing between two any adjacent cavity modes $\Delta\lambda$ is given by:

$$\Delta\lambda = \frac{\lambda^2}{L(n - \lambda \frac{dn}{d\lambda})} \quad (5)$$

The factor $dn/d\lambda$ is the dispersion relation. Two adjacent peaks $\lambda_1=564.7$ nm, $\lambda_2=575.2$ nm were selected from the TM signal to

calculate the effective optical path length. The mode spacing $\Delta\lambda$ is 10.5 nm. According to the dispersion of In_2O_3 crystal, the refractive index at the wavelength of 564.7 nm is about 2.039, and the relate $\lambda dn/d\lambda$ is about -0.371. We obtained the effective length L is about 12.53 μm . In addition, the side lengths of the measured In_2O_3 microwire $R_1 \approx 2$ μm and $R_2 \approx 2.84$ μm were determined by the SEM image (Fig. 2). According to the geometrical optics, if the resonant modes are cross-WGMs (Fig. 2(d)), the calculated $L' = 3 \times (2R_1 + R_2) = 20.52$ μm , which is much larger than the effective path length L (12.53 μm). If the resonant modes are quasi-WGMs (Fig. 2(e)), the obtained optical path length is $L' = 3 \times (R_1 + \frac{1}{2}R_2) = 10.26$ μm (mode 1) and $L' = 3 \times (R_2 + \frac{1}{2}R_1) = 11.52$ μm (mode 2). If the resonant modes originated from simple FPMs, the deduced optical path length is $L' = \sqrt{3}(R_1 + R_2) = 8.38$ μm . Obviously, the calculated optical path lengths L' based on the quasi-WGMs and FPMs are all smaller than the effective length L (12.53 μm). However, for the WGMs as shown in Fig. 2(c), the relevant optical path length is $L' = 6 \times [(\frac{1}{2}R_1)^2 + (\frac{1}{2}R_2)^2 - 2(\frac{1}{2}R_1)(\frac{1}{2}R_2)\cos\frac{2\pi}{3}] = 12.61$ μm , which is consistent with the calculated effective optical length L . So, it can be concluded that the measured resonant modes are attributed to the effect of the WGM type microwire cavity with irregular hexagonal cross section. Such resonant model with two different angle of TIR is different with the conventional WGMs, which also can effectively control the transmission and enhancement of a light field. In addition, it is noteworthy that additional resonant modes also exist in our PL spectra as shown in the enlarged view of the resonance peaks between 480 and 522 nm (Fig. 3(b)). This phenomenon may be related to irregular shape of the microwire structure. And we will also theoretically analyze this region in the following discussion.

To further investigate the optical modulations in the In_2O_3 microwire cavity, the photon energies of the resonant peaks were calculated by the WGM equation (1). We obtained the actual refractive indices (n_\perp and n_\parallel) of the In_2O_3 microcavity from the best fit of the WGM equation by varying N discretely and the radius R within the experimental error. This fitting process has been successfully applied to the calculation of other micro/nanostructure microcavities.²² The obtained scattered wavelength-dependent refractive indices can be fitted by using the Cauchy dispersion formula as follows:

$$n_\perp = 1.882 + \frac{77093.9}{\lambda^2} + \frac{2.462 \times 10^9}{\lambda^4} \quad (6)$$

$$n_\parallel = 1.869 + \frac{85227.1}{\lambda^2} + \frac{3.680 \times 10^9}{\lambda^4} \quad (7)$$

Fig. 3(c) shows the obtained refractive index curves from the above fitting process. It can be seen that the refractive indices for the TE and TM polarization at the same wavelength are almost the same, which is different from that of the previous reported other In_2O_3 crystals.⁹ The reason may be due to the difference of the anisotropic strain introduced during the crystal growth process. The two sets of integers shown in Fig. 3(b) are the interference orders of the resonant peaks. In addition, to further investigate the optical modulation and the quality of the whole microcavity along the c -axis, we performed the micro-luminescence scan in unpolarized and polarized detection. The scanning step is 1.0 μm . The obtained spatially resolved PL mapping along the c -axis is shown in Fig. 3(d)-(f). It can be seen

that two sets of WGMs with different periodicities are clearly resolved (Fig. 3(d)). These two sets of WGMs are well separated when the excitation laser polarization $E \perp c$ -axis and $E \parallel c$ -axis. The spectral maxima show slightly red shift, which indicates that the size of the hexagonal microcavity slightly increases along the c -axis. It is interesting to see that additional resonance modes also resolved in the spectra, which are dominated by the TM component. Such continuous obviously optical modulations demonstrate that the high quality and the strong light field regulation capability of the obtained In_2O_3 microwire optical cavity.

We then employ Finite Element Method (FEM) simulations to clarify the optical modes in such In_2O_3 microwire cavity with irregular hexagonal cross section. Because of the two-dimensional (2D) nature of the measured optical modes, we only need to simulate a 2D model with the same irregular hexagonal cross section as the fabricated microwire shown in Fig. 2(a) to simplify our calculation. In our simulations, the modeled microcavity is placed inside a simulation box surrounded by the perfect matched layers boundaries to absorb the scattered electromagnetic fields. The dimensions of the simulated microcavity are all same as the fabricated irregular hexagonal samples (Fig. 2(a)) with the two side lengths as 2 μm and 2.84 μm , respectively. The refractive index of In_2O_3 microcavity is chosen from the values shown in Fig. 3(c). The background medium is set as air. A magnetic or electric current source is put inside the 2D In_2O_3 microcavity to excite the optical modes in TE or TM polarization. The calculated radiation spectra of the current source are shown in Fig. 4(b) and (d). While the radiation wavelength of the line source matches that of the resonance modes of the microcavity, its radiation will be obviously enhanced. And the radiation peaks are the unambiguous signatures of the optical modes excited in the In_2O_3 microcavity. We can see that FEM simulations perfectly match the experimental results (Fig. 4(a) and (c)). To further understand the nature of these optical modes, we have also studied our microcavity based on the eigenmode analysis simulation. Fully taking the dispersive property of In_2O_3 into account, the eigenmode analysis solver of COMSOL Multiphysics employ an iterative method to gradually approach the eigenmodes and finally get the convergent results. Both the field patterns and resonance wavelengths (inset) of the optical modes are shown in Fig. 5. The field patterns of Fig. 5(c-e, i-k) clearly exhibit the pictures of WGM (type I). Obviously standing waves are formed with a quasi hexagonal optical path inside the In_2O_3 . And the calculated resonance wavelengths of these modes also match well with the spectra peaks shown in Fig. 5(a, b). The simulation results fit well with theoretical prediction of WGM based on the plane wave interference model. Meanwhile the quasi-WGM (type III, Fig. 5(f-g, l-m)) and FPM (type IV, Fig. 5(h, n)) can also exist in such microwire. Because of the low quality factor or excitation condition, there are no obvious features of quasi-WGM and FPM in the measured spectra shown in Fig. 4. Nevertheless, their resonance wavelengths indeed locate around the spectra peaks of the WGMs. In the above discussion, we have mentioned that the two quasi-WGM modes have different optical path. It will lead to the splitting of their resonance wavelengths which has been demonstrated by FEM simulations as shown in Fig.5 (f, g, h, m).

Such effect is due to the broken hexagonal symmetry of irregular hexagonal cavity. The studies will lay a theoretical and experimental foundation for the design of optical resonators with non-strict symmetric structures.

Conclusion

In summary, we have developed a facile solution and catalyst-free route to grow single crystalline In_2O_3 microwires with irregular hexagonal cross sections. Interestingly, such microwires can effectively control the light field in low dimensions. We systematically investigate the resonant modes in microwire optical cavities with irregular hexagonal cross sections for the first time. Compared to the traditional hexagonal WGM microcavity, the broken hexagonal symmetry of the geometric configuration will lead to quite different features of optical modulation. WGMs with different polarization were directly observed at room temperature. Theoretical analyses based on the plane wave model and FEM simulations agreed well with the experimental results and provide a further understanding of the low dimensional optical modulations. Such In_2O_3 microwire optical cavities with irregular cross sections may be an ideal test-bed for the development of novel cavity-based optical devices.

Acknowledgements

This work was supported financially by the NSFC (61378074, 61108059). Shanghai Rising-star Program (A type 14QA1404000). Shanghai Science and Technology Committee (Grant No. 14PJ1401200).

Notes and references

1. F. Qian, Y. Li, S. Gradecak, H. G. Park, Y. Dong, Y. Ding, Z. L. Wang and C. M. Lieber, *Nat. Mater.*, 2008, **7**, 701.
2. C. Grivas, C. Li, P. Andreakou, P. Wang, M. Ding, G. Brambilla, L. Manna and P. Lagoudakis, *Nat. Commun.*, 2013, **4**, 2376.
3. M. Law, D. J. Sirbuly, J. C. Johnson, J. Goldberger, R. J. Saykally and P. D. Yang, *Science*, 2004, **305**, 1269.
4. J. Huang, S. Chu, J. Y. Kong, L. Zhang, C. M. Schwarz, G. P. Wang, L. Chernyak, Z. H. Chen, J. L. Liu, *Adv. Optical Mater.*, 2013, **1**, 179.
5. L. Maleki, A. A. Savchenko, A. B. Matsko and V. S. Ilchenko, *Proc. SPIE*, 2004, **5435**, 178.
6. F. X. Gu, L. Zhang, X. F. Yin, L. M. Tong, *Nano Lett.*, 2008, **8**, 2757.
7. T. Nobis, E. M. Klaidashev, A. Rahm, M. Lorenz and M. Grundmann, *Phys. Rev. Lett.*, 2004, **93**, 103903.
8. P. M. Coulon, M. Hugues, B. Alloing, E. Beraudo, M. Leroux and J. Zuniga-Perez, *Opt. Express*, 2012, **20**, 18707.
9. H. X. Dong, Z. H. Chen, L. X. Sun, J. Lu, W. Xie, H. H. Tan, C. Jagadish and X. C. Shen, *Appl. Phys. Lett.*, 2009, **94**, 173115.
10. H. Zhu, S. F. Yu, Q. J. Wang, C. X. Shan and S. C. Su, *Opt. Lett.*, 2013, **38**, 1527.
11. W. Xie, H. X. Dong, S. F. Zhang, L. X. Sun, W. H. Zhou, Y. J. Ling, J. Lu, X. C. Shen and Z. H. Chen, *Phys. Rev. Lett.*, 2012, **108**, 166401.
12. H. X. Dong, Y. Liu, J. Lu, Z. H. Chen, J. Wang and L. Zhang, *J. Mater. Chem. C*, 2013, **1**, 202.
13. H. X. Dong, L. X. Sun, W. Xie, W. H. Zhou, X. C. Shen and Z. H. Chen, *J. Phys. Chem. C*, 2010, **114**, 17369.
14. Z. W. Pan, Z. R. Dai and Z. L. Wang, *Science*, 2001, **291**, 1947.
15. T. Lim, S. Lee, M. Meyyappan and S. Ju, *ACS Nano*, 2011, **5**, 3917.
16. C. J. Chen, W. L. Xu and M. Y. Chern, *Adv. Mater.*, 2007, **19**, 3012.

17. H. Q. Yang, R. G. Zhang, H. X. Dong, J. Yu, W. Y. Yang and D. C. Chen, *Cryst. Growth Des.*, 2008, **8**, 3154.
18. Y. Lei and W. K. Chim, *J. Am. Chem. Soc.*, 2005, **127**, 1487.
19. S. Ghosh, K. Das, G. Sinha, J. Lahtinen and S. K. De, *J. Mater. Chem. C*, 2013, **1**, 5557. 50
20. Y. B. Li, Y. Bando and D. Golberg, *Adv. Mater.*, 2003, **15**, 581.
21. M. R. Shi, F. Xu, K. Yu, Z. Q. Zhu and J. H. Fang, *J. Phys. Chem. C*, 2007, **111**, 16267.
22. C. Czekalla, C. Sturm, R. Schmidt-Grund, B. Q. Cao, M. Lorenz and M. Grundmann, *Appl. Phys. Lett.*, 2008, **92**, 241102. 55

15 60

20 65

25 70

30 75

35 80

40 85

45

90

95

100

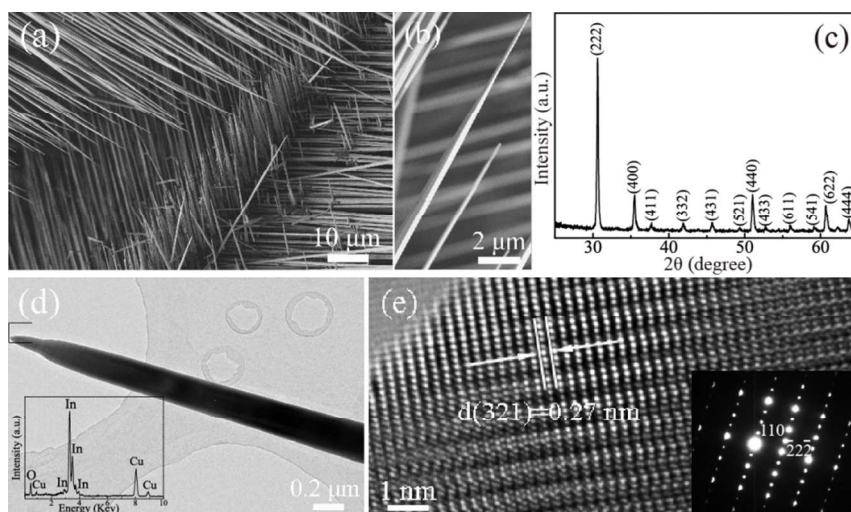


Fig. 1 (a) Typical SEM image of as-prepare In_2O_3 microwires grown on a quartz substrate at high density. (b) High-magnification SEM image of the In_2O_3 microwires. (c) XRD pattern of the In_2O_3 microwires measured using Cu ka radiation. (d) TEM image and EDS spectrum (inset) of one single In_2O_3 microwire. (e) HRTEM image and the corresponding SAED pattern (inset) from the rectangular region marked in (d).

5

10

15

20

25

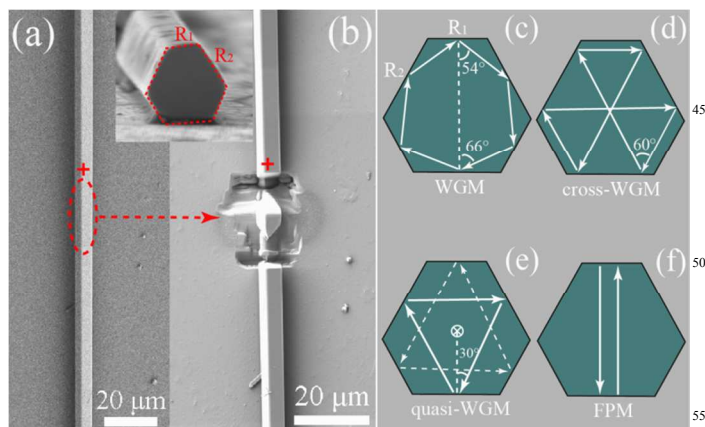


Fig. 2 (a) SEM image of the microwire and the focused laser spot is marked by a red cross. (b) SEM image of the microwire etched by focused ion beam. The inset shows the cross section of the microwire cavity. (c-f) The diagrams of four kinds of resonant modes, (c) WGM, (d) cross-WGM, (e) quasi-WGM and (f) FPM, formed in the microwire cavity.

60

90

65

95

70

100

75

105

80

110

85

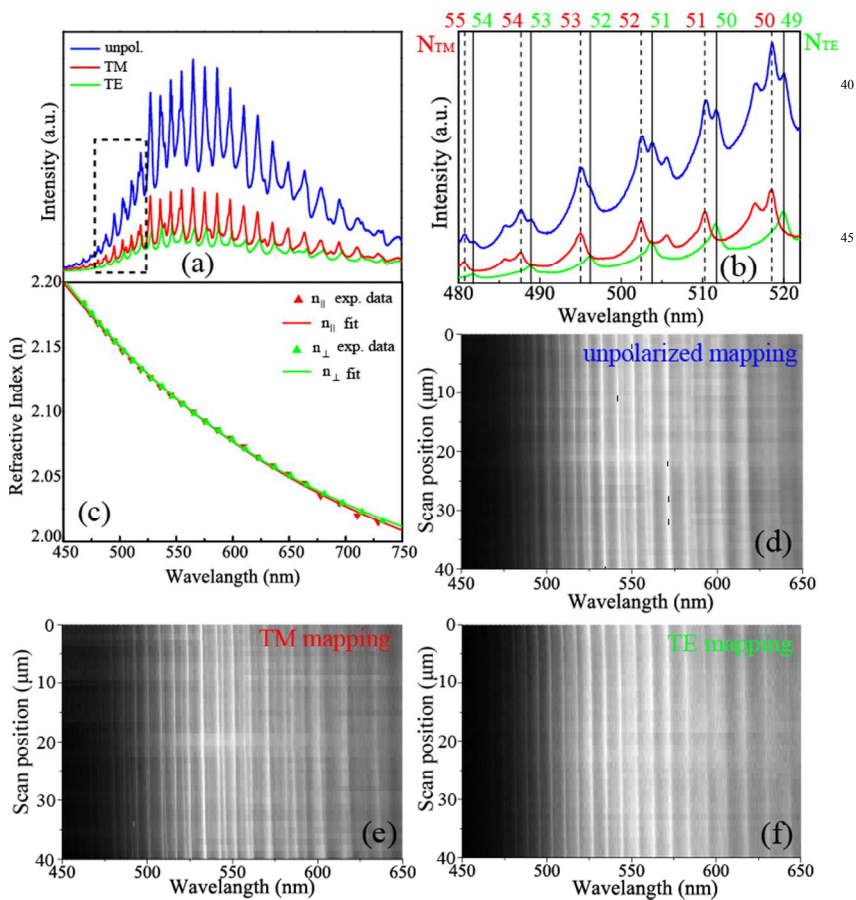
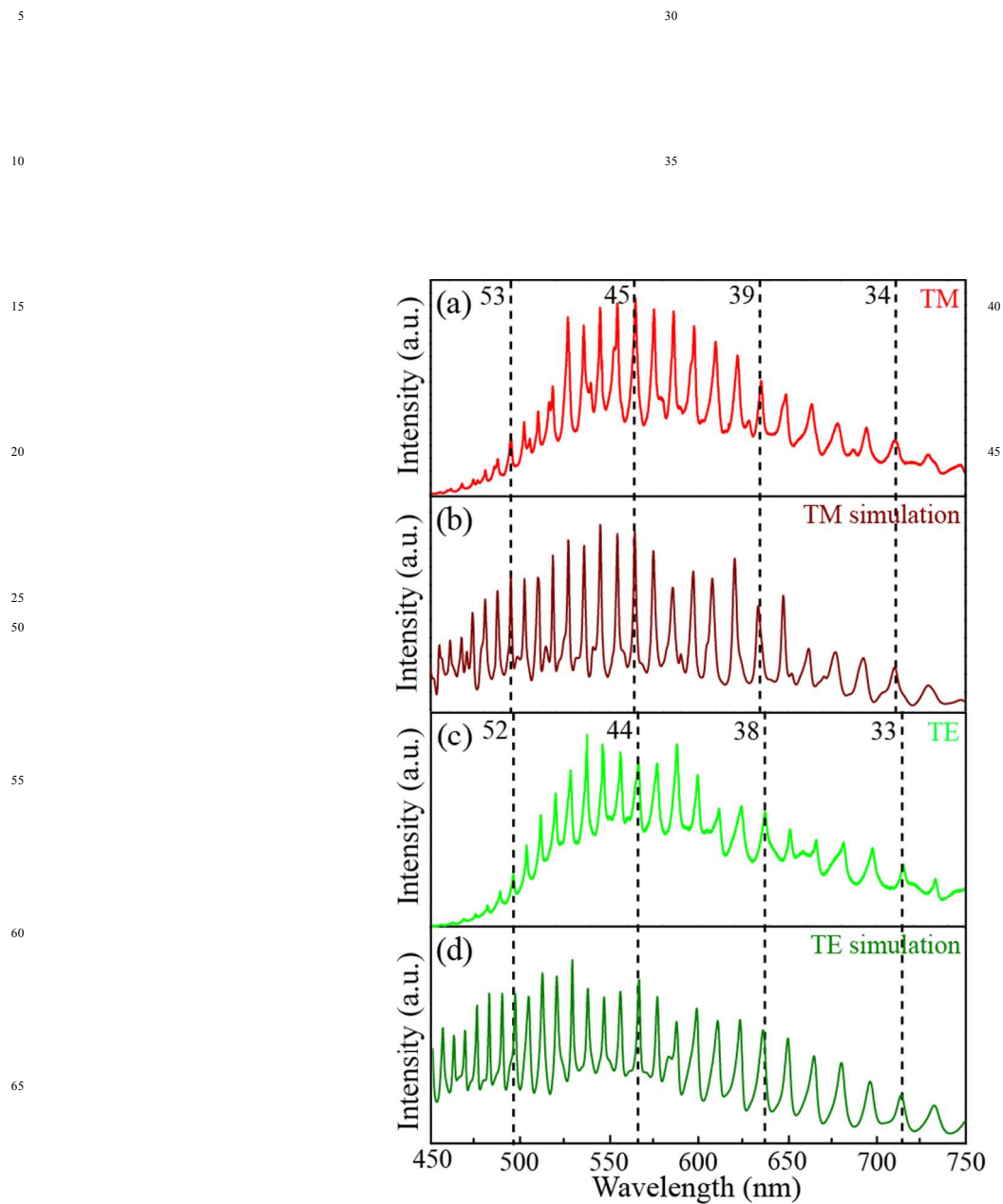


Fig. 3 (a) PL spectra with unpolarized (blue curve), TM polarized (red curve) and TE polarized (green curve) in the visible region. (b) An enlarged view of the resonance peaks between 480 to 522 nm from the dashed rectangular region marked in (a). (c) The simulated wavelength dependent refractive indices of the In_2O_3 microwire for both n_{\perp} and n_{\parallel} . (d-f) Spatially resolved PL mapping of the In_2O_3 microwire along the c-axis with unpolarized, TM and TE detection, respectively.



70 **Fig. 4** The measured PL spectra (a, c) and FEM simulated radiation spectra (b, d) of single In_2O_3 microwire with an irregular hexagonal cross section for both TM (a, b) and TE (c, d) polarization.

75

85

80

90

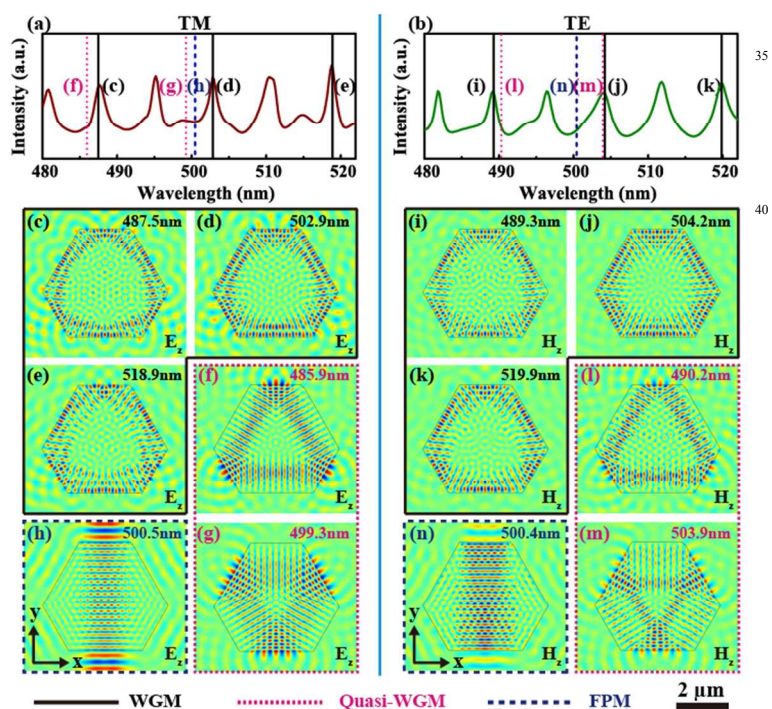


Fig. 5 Simulated radiation spectra (a-b) and E_z (c-h) and H_z (i-n) field distributions of some resonance modes inside the irregular hexagonal microcavity for TE (a, c-h) and TM (b, i-n) polarization. These modes can be categorized into WGM (c-e, i-k), quasi WGM (f-g, l-m) and FP mode (h, n) with their resonance wavelengths shown as insets. The two side lengths of the microwire are $2 \mu\text{m}$, $2.84 \mu\text{m}$ and the scale bar is $2 \mu\text{m}$.